Energy Optimal Distributed Beamforming using Unmanned Vehicles

Arjun Muralidharan and Yasamin Mostofi

***Abstract*—In this paper, we consider a team of unmanned vehicles that are tasked with distributed transmit beamforming (virtual antenna array placement and design), in order to cooperatively transmit information to a remote station in realistic communication environments. We are interested in the energy-aware (both motion and communication energy) co-optimization of robotic paths and transmission powers for cooperative transmit beamforming under a reception quality requirement. We first consider the case where the channel is known. For this case, we propose an efficient approach for getting arbitrarily close to the optimum solution, which involves solving a series of multiple-choice knapsack problems. We then extend our analysis and methodology to the case where the channel is not known. The robots then probabilistically predict the channel at unvisited locations and integrate it with path planning and decision making for energy-aware distributed transmit beamforming. Finally, we extensively confirm our proposed approach with several simulation results with real channel parameters. Our results highlight the underlying trends of the optimum strategy and indicate a considerable energy saving.**

I. Introduction

Networked robotic systems have been the focus of considerable research in recent years. Such systems are envisioned to carry out tasks such as search and rescue, surveillance, exploration, and sensing of the environment. Maintaining proper connectivity or transferring data to a remote station is a key enabling factor in many of these tasks, and the mobility of the unmanned nodes can play an important role in achieving proper connectivity by actively moving to places better for communication. Since unmanned vehicles typically have a limited energy budget, energy efficiency is of prime importance in these systems. Thus, energy-aware co-optimization of communication and motion strategies is needed to truly realize the full potentials of these systems, which is the main motivation for this paper.

Co-optimization of motion and communication strategies in robotic systems has recently attracted attention of both communication and robotics communities [2]–[10]. For instance, in [2], a node co-optimizes its motion speed and communication transmission rate, while a number of nodes utilize their mobility to form a communication relay network in [3]. In [6], robots act as collaborative relay beamformers, without considering motion energy costs. In [5], robots utilize mobility to maintain an optimal communication chain between a source and a destination node. In [11], the probability density function (pdf) of the distance traveled before the robot gets connected is derived.

On the communication side, distributed transmit beamforming is a cooperative communication strategy where a number of fixed transmitters cooperate to emulate a virtual centralized antenna array. For instance, consider the case where a node needs to transmit information to a remote station. If the corresponding link quality is not good, successful communication may not be possible. Instead, a number of transmitters can perform transmit beamforming, which means co-phasing and properly weighing their transmitted signals to communicate the same message while maintaining the same total communication power. In this manner, transmit beamforming creates an equivalent strong link to the receiving node. Transmit beamforming was originally proposed in the context of multiple co-located antennas for improving transmission quality of communication systems. More recently, it has been extensively studied in the context of fixed nodes that are spatially distributed over a given area [12], [13]. Then, the nodes align their transmission phases such that the wireless signals merge constructively at the remote station, thus providing dramatic gains in the signal to noise ratio (SNR). Using unmanned vehicles creates new possibilities for distributed transmit beamforming by enabling the transmitters to position themselves in better locations for beamforming, thus improving the overall performance significantly. However, several challenges for motion and communication co-planning need to be addressed before realizing this vision, which is the main motivation for this paper.

In this paper, we are interested in an *energy-aware distributed transmit beamforming using unmanned vehicles*. More specifically, we consider the problem where a team of unmanned vehicles are tasked with cooperatively transmitting information, via distributed transmit beamforming, to a remote station while minimizing the total energy consumption including both motion and communication energy costs. We are then interested in characterizing the optimal motion and communication strategies of the robots, including the optimization of the transmit power and robot paths. Fig. 1 shows an illustration of distributed robotic transmit beamforming.

As compared to the existing literature on distributed beamforming, most work are not concerned with unmanned vehicles and the resulting challenges in terms of path planning and motion energy. In [6], where robots act as collaborative relay beamformers, motion energy-related issues are not considered, resulting in a different problem formulation. Moreover, there is no channel learning and prediction. Finally, the motion of the

This work is supported in part by NSF NeTS award 1321171 and NSF RI award 1619376. A small part of this work has appeared in [1]. As compared to the conference version, which only considered motion energy consumption, this paper considers both communication and motion energy consumption, resulting in a different formulation and a more extensive analysis/optimization.

The authors are with the Department of Electrical and Computer Engineering, University of California Santa Barbara, Santa Barbara, CA 93106, USA email: {arjunm, ymostofi}@ece.ucsb.edu.

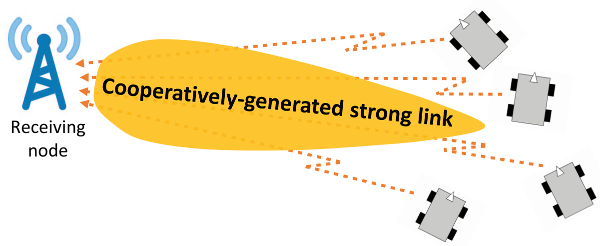

Fig. 1: Distributed robotic transmit beamforming. The robots can cooperatively generate a strong communication link by optimizing their locations.

relays is myopic, and they can get stuck in a local minimum. In [14], the robots self organize to form a distributed pattern for beamforming. However, an unrealistic path loss-only model is considered and the operation is not energy-aware. Overall, this paper is different from the existing work on cooperative beamforming in that it deals with the *co-optimization of motion and communication* strategies, while considering 1) the *total energy consumption*, 2) *channel learning and prediction* in realistic communication environments, and 3) the *coupled decision making* that arises when dealing with multi-agent systems. Fig. 2 shows an example of such a scenario.

In Section II, we introduce the motion and communication energy cost models and briefly review distributed transmit beamforming as well as wireless channel modeling and prediction. In Section III, we consider the scenario where the robots do not satisfy the reception quality requirement from their initial positions when employing distributed transmit beamforming. We are then interested in determining the optimum paths of the robots such that the reception requirement is met with minimum motion energy cost. In Section IV, we then incorporate communication energy cost into our framework, i.e, we minimize the total energy cost (both motion and communication) while satisfying the reception quality requirement. We are then interested in the co-optimization of robotic paths and transmission powers for cooperative transmit beamforming. In Section V, we confirm our proposed approach with extensive simulation results using channel parameters obtained from real measurements [15]. Our results indicate a considerable energy saving.

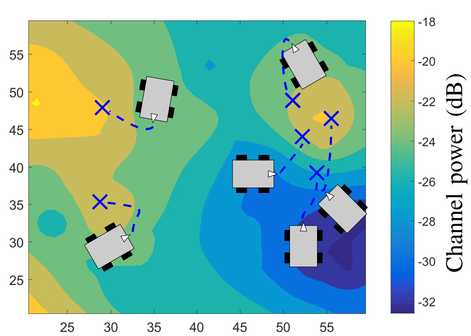

Fig. 2: Distributed robotic beamforming – The robots move to locations (marked by empty circles) better for satisfying the cooperative connectivity requirement, while minimizing the total energy consumption (both motion and communication). Readers are referred to the color pdf for better viewing of the superimposed channel.

II. Problem Setup

In this section we first introduce our energy consumption models for both motion and communication. We then review distributed transmit beamforming and the corresponding power gains that it provides. Finally, we briefly summarize probabilistic modeling and prediction of wireless channels.

A. Motion Energy Model

In this paper, we adopt a model where the motion energy consumption is proportional to the distance traveled, similar to the one adopted in [16], [17]. Thus, motion energy $= \kappa_M d$, where d is the distance traveled by the robot and κ_M is a constant that depends on the environment (e.g., friction coefficient, terrain) and the mass of the vehicle. This model is a good match for wheeled robots (see [16] for discussion).

B. Communication Energy Model

We consider a generic model of communication rate of the form $R = \eta_1 B \log_2\left(1+\eta_2 \frac{P_R}{N_0}\right)$, where $\eta_1, \eta_2 \leq 1$ are constants, B is the available bandwidth, P_R is the received power and N_0 is the noise power.[1] For capacity approaching codes (such as turbo codes and LDPC), the constants for a binary symmetric channel correspond to $\eta_1 = 1-\varepsilon$ and $\eta_2 = 1$ where ε is the multiplicative gap to capacity [18]. For an uncoded MQAM modulation scheme with a target bit error rate of BER_{th}, we obtain $\eta_1 = 1$ and $\eta_2 = 1.5/\ln(5\text{BER}_{\text{th}})$ [19]. The communication energy incurred in transmitting l bits of data can then be expressed as

$$\text{Communication Energy} = \underbrace{\frac{l}{\eta_1 B \log_2\left(1+\eta_2 \frac{P_R}{N_0}\right)}}_{\text{time to transmit } l \text{ bits}} P_0, \quad (1)$$

where P_0 is the transmit power.

C. Distributed Transmit Beamforming

Distributed transmit beamforming is a form of cooperative communication where several nodes that are distributed in a given space emulate a centralized antenna array [12]. The nodes simultaneously transmit the same message with phases such that the signals combine constructively at the remote station. Channel state information (CSI), i.e., information about the channel, is required at the transmitters for the implementation of distributed transmit beamforming.

Consider N robots in an environment. Let $h_i = \alpha_i e^{j\theta_i}$ denote the complex baseband channel from robot i to the remote station with α_i and θ_i denoting the channel amplitude and phase respectively. Ideally, node i transmits $w_i s(t)$ where $w_i = \rho_i e^{-j\theta_i}$ is the complex beamforming weight and $s(t)$ is the complex baseband signal to be transmitted. As can be seen, setting $\angle w_i = -\angle h_i = -\theta_i$ is the crucial step in obtaining a constructive interference and thus beamforming gains. The received signal is then $(\sum_{i=1}^{N} h_i w_i) s(t) = \sum_{i=1}^{N} (\alpha_i \rho_i) s(t)$ resulting in the received SNR of $\frac{P_0 (\sum_{i=1}^{N} \alpha_i \rho_i)^2}{N_0}$ where the transmit power of robot i is $\rho_i^2 P_0$. Constraining $\rho_i \leq 1$ imposes a maximum power of P_0 on each node. We stress here the difference from the traditional centralized transmit beamforming where a total transmit power is enforced, i.e. $\sum_{i=1}^{N} \rho_i^2 \leq 1$. However, in distributed beamforming, the

[1] Note that the communication rate is adaptive as it is a function of the received power.

nodes are separated and have their own power supply. We thus impose individual power constraints instead. Note that the position of node i affects α_i, the corresponding channel amplitude, and therefore the overall received SNR. Thus, by properly designing robotic paths and transmit power (ρ_i), using unmanned vehicles can significantly improve distributed transmit beamforming, as we shall see in this paper.

D. Overview of Channel Modeling and Prediction

1) Probabilistic Channel Modeling [19]: A communication channel is well modeled as a multi-scale random process with three major dynamics: path loss, shadowing and multipath fading [19]. Let $\Gamma(q_1) = |h(q_1)|^2$ represent the received channel power from a transmitter at location $q_1 \in \mathcal{W}$ ($\mathcal{W} \subseteq \mathbb{R}^2$ is the workspace) to the remote station located at q_b. The received channel power in dB, $\Gamma_{\text{dB}}(q_1) = 10\log_{10}\Gamma(q_1)$, can be expressed as $\Gamma_{\text{dB}}(q_1) = \Gamma_{\text{PL,dB}}(q_1) + \Gamma_{\text{SH,dB}}(q_1) + \Gamma_{\text{MP,dB}}(q_1)$ where $\Gamma_{\text{PL,dB}}(q_1) = K_{\text{dB}} - 10 n_{\text{PL}} \log_{10}\|q_1 - q_b\|$ is the distance-dependent path loss with n_{PL} representing the path loss exponent, and $\Gamma_{\text{SH,dB}}$ and $\Gamma_{\text{MP,dB}}$ are random variables denoting the impact of shadowing and multipath respectively. $\Gamma_{\text{SH,dB}}(q_1)$ is best modeled as a Gaussian random variable with an exponential spatial correlation, i.e., $\mathbb{E}\left\{\Gamma_{\text{SH,dB}}(q_1)\Gamma_{\text{SH,dB}}(q_2)\right\} = \nu_{\text{SH}} e^{-\|q_1-q_2\|/\beta_{\text{SH}}}$ where ν_{SH} is the shadowing power and β_{SH} is the decorrelation distance.

2) Realistic Channel Prediction [10], [20]: Let $\vartheta = [K_{\text{dB}}\ n_{\text{PL}}]^{\text{T}}$ denote the vector of path loss parameters. Let $\Gamma_{q,\text{dB}}$ represent the vector of m a priori-gathered received channel power measurements (in dB) from the same environment, and $q = [q_1 \cdots q_m]^{\text{T}}$ denote the vector of the corresponding positions.

Lemma 1 (See [20] for proof): A Gaussian random vector, $\Gamma_{\text{dB}}(p) = [\Gamma_{\text{dB}}(p_1) \cdots \Gamma_{\text{dB}}(p_k)]^{\text{T}} \sim \mathcal{N}\left(\overline{\Gamma}_{\text{dB}}(p), C_{\text{dB}}(p)\right)$ can best characterize the vector of channel power (in the dB domain) when transmitting from unvisited locations $p = [p_1 \cdots p_k]^{\text{T}}$, with the mean and covariance matrix given by $\overline{\Gamma}_{\text{dB}}(p) = \mathbb{E}\left\{\Gamma_{\text{dB}}(p) \mid \Gamma_{q,\text{dB}}, \hat{\vartheta}, \hat{\beta}_{\text{SH}}, \hat{\nu}_{\text{SH}}, \hat{\nu}_{\text{MP}}\right\} = G_p\hat{\vartheta} + \Psi_{p,q}\Phi_q^{-1}\left(\Gamma_{q,\text{dB}} - G_q\hat{\vartheta}\right)$ and $C_{\text{dB}}(p) = \mathbb{E}\Big\{\left(\Gamma_{\text{dB}}(p) - \overline{\Gamma}_{\text{dB}}(p)\right)\left(\Gamma_{\text{dB}}(p) - \overline{\Gamma}_{\text{dB}}(p)\right)^{\text{T}} \mid \Gamma_{q,\text{dB}}, \hat{\vartheta}, \hat{\beta}_{\text{SH}}, \hat{\nu}_{\text{SH}}, \hat{\nu}_{\text{MP}}\Big\} = \Phi_p - \Psi_{p,q}\Phi_q^{-1}\Psi_{p,q}^{\text{T}}$ respectively, where $G_p = [\mathbf{1}_k\ \ -D_p]$, $G_q = [\mathbf{1}_m\ \ -D_q]$, $\mathbf{1}_m$ ($\mathbf{1}_k$) represents the m-dimensional (k-dimensional) vector of all ones, $D_q = \left[10\log_{10}(\|q_1 - q_b\|)\ \cdots\ 10\log_{10}(\|q_m - q_b\|)\right]^{\text{T}}$, $D_p = \left[10\log_{10}(\|p_1 - q_b\|)\ \cdots\ 10\log_{10}(\|p_k - q_b\|)\right]^{\text{T}}$ and q_b is the position of the remote station. Furthermore, Φ_q, Φ_p and $\Psi_{p,q}$ denote matrices with entries $\left[\Phi_q\right]_{i_1,i_2} = \hat{\nu}_{\text{SH}} e^{-\|q_{i_1}-q_{i_2}\|/\hat{\beta}_{\text{SH}}} + \hat{\nu}_{\text{MP}}\,\delta_{i_1 i_2}$, $\left[\Phi_p\right]_{j_1,j_2} = \hat{\nu}_{\text{SH}} e^{-\|p_{j_1}-p_{j_2}\|/\hat{\beta}_{\text{SH}}} + \hat{\nu}_{\text{MP}}\delta_{j_1,j_2}$ and $\left[\Psi_{p,q}\right]_{j_1,i_1} = \hat{\nu}_{\text{SH}}\ e^{-\|p_{j_1}-q_{i_1}\|/\hat{\beta}_{\text{SH}}}$, where $i_1, i_2 \in \{1, \cdots, m\}$, $j_1, j_2 \in \{1, \cdots, k\}$ and $\delta_{i,j} = \begin{cases} 1, & \text{if } i = j \\ 0, & \text{else} \end{cases}$. Moreover, ϑ, β_{SH}, ν_{SH} and ν_{MP} denote the path loss parameters, the decorrelation distance of shadowing, the power of shadowing (in dB) and the power of multipath (in dB) respectively. The $\hat{}$ symbol denotes the estimate of the corresponding parameter.

The underlying parameters can be estimated based on the a priori measurements as well. See [20] for more details on the estimation of the underlying parameters and the performance of this framework with real data and in different environments.

III. Motion Energy-Aware Cooperative Robotic Beamforming

Consider the case where the robots are distributed over the space such that the required cooperative received SNR is not satisfied. The robots thus need to move to new positions that satisfy the cooperative connectivity requirement while minimizing the motion energy consumption. We start by looking at the case of perfect channel knowledge (i.e., the robots know the uplink channel quality for transmission from any unvisited location), and show how this problem can be optimally solved by posing it as a multiple-choice knapsack problem. We then extend our analysis to the stochastic case where the nodes predict the channel based on a small number of a priori channel samples, as discussed in Section II-D2. In this section we focus on motion energy minimization, assuming a non-adaptive communication transmit power case.

A. Perfect Channel Knowledge

The perfect channel knowledge assumption would be a good approximation for environments where path loss is dominant and channel has a low variance around path loss. In our case, this serves as a starting point for our analysis, which will then be extended to the general case of an unknown channel. Consider N robots in a workspace $\mathcal{W} \subseteq \mathbb{R}^2$. Let $d_i(x_i) = ||x_i - x_i^0||_2$ be the distance traveled by robot i with x_i^0 and x_i denoting the initial and final position respectively. Let $h(x_i) = \alpha(x_i)e^{j\theta(x_i)}$ be the uplink channel from position x_i to the remote station with $\alpha(x_i)$ and $\theta(x_i)$ denoting the channel amplitude and phase respectively.

Since communication cost is not penalized in this setup, the optimal thing for the nodes would be to maximize the SNR at the remote station, subject to the individual power constraints. We then set $\rho_i = 1$, which corresponds to each node transmitting at the maximum allowed power, and the complex beamforming weight as $w_i = e^{-j\theta(x_i)}$, for the i^{th} node. The received signal power, after beamforming, is then given by $P_R = P_0\left(\sum_{i=1}^N \alpha(x_i)\right)^2$.

A Quality of Service (QoS) requirement, such as a target bit error rate, would result in a minimum required received power at the remote station, which we denote as $P_{R,\text{th}}$. We then need $P_R = P_0\left(\sum_{i=1}^N \alpha(x_i)\right)^2 \geq P_{R,\text{th}}$ or equivalently $\sum_{i=1}^N \alpha(x_i) \geq \sqrt{\frac{P_{R,\text{th}}}{P_0}}$, which results in the following optimization problem,

$$\begin{aligned} \underset{x}{\text{minimize}} \quad & \kappa_M \sum_i d_i(x_i) \\ \text{subject to} \quad & \sum_i \alpha(x_i) \geq \alpha_{R,\text{th}} \\ & x_i \in \mathcal{N}(x_i^0),\ i = 1, \cdots, N, \end{aligned} \tag{2}$$

where $\alpha_{R,\text{th}} = \sqrt{\frac{P_{R,\text{th}}}{P_0}}$, $\mathcal{N}(x_i^0) \subseteq \mathcal{W}$ is the neighborhood around x_i^0 that the i^{th} node is constrained to stay in, and $x = [x_1 \cdots x_N]^{\text{T}}$ are the final positions of the robots.

Optimal Solution: We next show how to repose the optimization problem of (2) as a multiple-choice knapsack problem, which is a well studied problem in the computer science literature and can be solved optimally [21]. We first discretize our workspace $\mathcal{W}$ into M cells with centers $r_j \in \mathcal{W}, \quad \text{for } j \in \{1, \cdots, M\}$. The motion cost is then given by $J_{\text{MEMP}}(\{z_{ij}\}) = \kappa_M \sum_{i=1}^{N} \sum_{j\in\mathcal{N}_i} d_i(r_j) z_{ij}$ and the optimization problem of (2) can be reformulated as

$$\begin{aligned} \underset{\{z_{ij}\}}{\text{minimize}} \quad & J_{\text{MEMP}}(\{z_{ij}\}) \\ \text{subject to} \quad & \sum_i \sum_{j\in\mathcal{N}_i} \alpha(r_j) z_{ij} \geq \alpha_{R,\text{th}} \\ & \sum_{j\in\mathcal{N}_i} z_{ij} = 1,\ z_{ij} \in \{0,1\},\ \forall\, j \in \mathcal{N}_i,\ \forall\, i, \end{aligned} \tag{3}$$

where $d_i(r_j)$ is the distance to cell j for robot i, $\alpha(r_j)$ is the channel amplitude from cell j to the remote station and $\mathcal{N}_i \subseteq \{1, \cdots, M\}$ is the set of cells present in $\mathcal{N}(x_i^0)$. A value of $z_{ij} = 1$ implies that robot i chooses to move to cell j. We refer to this problem as the Motion Energy Minimization Problem (MEMP), with the optimal value of $J_{\text{MEMP}}^{\text{OPT}}$.

Lemma 2: MEMP of (3) can be posed as a multiple-choice knapsack problem (MCKP).

Proof: Define $\{\pi_{ij}\}$ and $\{\varpi_j\}$ as $\pi_{ij} = \max_{k\in\mathcal{N}_i} d_i(r_k) - d_i(r_j)$ and $\varpi_j = \max_k \alpha(r_k) - \alpha(r_j)$. We have $\sum_{i=1}^{N}\sum_{j\in\mathcal{N}_i} \pi_{ij} z_{ij} = \sum_{i=1}^{N} \max_{k\in\mathcal{N}_i} d_i(r_k) \sum_{j\in\mathcal{N}_i} z_{ij} - \sum_{i=1}^{N}\sum_{j\in\mathcal{N}_i} d_i(r_j) z_{ij} = \sum_{i=1}^{N} \max_{k\in\mathcal{N}_i} d_i(r_k) - \sum_{i=1}^{N}\sum_{j\in\mathcal{N}_i} d_i(r_j) z_{ij}$, where the second equality follows for any feasible solution since $\sum_{j=1}^{M} z_{ij} = 1$. Similarly, $\sum_{i=1}^{N}\sum_{j\in\mathcal{N}_i} \varpi_j z_{ij} = N \max_k \alpha(r_k) - \sum_i \sum_{j\in\mathcal{N}_i} \alpha(r_j) z_{ij}$. MEMP of (3) can then be posed as

$$\begin{aligned} \underset{\{z_{ij}\}}{\text{maximize}} \quad & \sum_i \sum_{j\in\mathcal{N}_i} \pi_{ij} z_{ij} \\ \text{subject to} \quad & \sum_i \sum_{j\in\mathcal{N}_i} \varpi_j z_{ij} \leq c \\ & \sum_{j\in\mathcal{N}_i} z_{ij} = 1,\ z_{ij} \in \{0,1\},\ \forall\, j \in \mathcal{N}_i,\ \forall\, i, \end{aligned} \tag{4}$$

where $c = N \max_k \alpha(r_k) - \alpha_{R,\text{th}}$. ■

Equation (4) is the standard form of the multiple-choice knapsack problem (MCKP). Although MCKP is NP-hard, the true solution can be efficiently found for several cases that arise in practice [21]. In this paper, we thus utilize the minimal algorithm developed by Pisinger [21] to optimally solve the resulting MCKP.

Remark 1: Let $J_{\text{MCKP}}^{\text{OPT}}$ denote the optimal value of the objective function of (4). The optimal values of the two formulations (3) and (4) are then related as follows:

$$J_{\text{MEMP}}^{\text{OPT}} = \kappa_M \Big(\sum_i \max_{k\in\mathcal{N}_i} d_i(r_k) - J_{\text{MCKP}}^{\text{OPT}} \Big).$$

B. Probabilistic Channel Prediction

In realistic scenarios, the uplink channel values in transmission from unvisited locations may not be known to the robots a priori. We next consider this realistic case. The robots then utilize the stochastic prediction approach of Section II-D2 to predict the channel strength when transmitting from an unvisited location, using a small number of a priori channel samples in the same environment.[2] Optimization of path planning for cooperative beamforming can then be posed as follows in this case,

$$\begin{aligned} \underset{x}{\text{minimize}} \quad & \kappa_M \sum_i d_i(x_i) \\ \text{subject to} \quad & \Pr\Big(\sum_i \alpha(x_i) < \alpha_{R,\text{th}} \Big) < \Pr_{\text{out}} \\ & x_i \in \mathcal{N}(x_i^0),\ i = 1, \cdots, N, \end{aligned} \tag{5}$$

where $\Pr(.)$ denotes the probability of the argument, $\alpha(x_i) = \sqrt{\Gamma(x_i)}$ is the random variable that represents the received channel amplitude when the i^{th} node transmits from x_i, and $\Pr_{\text{out}}$ is the maximum tolerable outage probability.

As discussed in Section II, the predicted channel power (in dB) when transmitting from unvisited locations $x = [x_1 \cdots x_N]^{\text{T}} \in \mathcal{W}^N$ can be represented as a Gaussian random vector $\Gamma_{\text{dB}}(x) \sim \mathcal{N}(\overline{\Gamma}_{\text{dB}}(x), C_{\text{dB}}(x))$, where $\overline{\Gamma}_{\text{dB}}(x)$ and $C_{\text{dB}}(x)$ are the estimated mean and covariance matrix respectively. Thus, the channel amplitude at locations x, $\alpha(x) = [\alpha(x_1) \cdots \alpha(x_N)]^{\text{T}} = \Big[\sqrt{\Gamma(x_1)} \cdots \sqrt{\Gamma(x_N)}\Big]^{\text{T}}$ is a lognormal random vector, i.e., $[20\log_{10}\alpha(x_1) \cdots 20\log_{10}\alpha(x_N)]^{\text{T}} \sim \mathcal{N}(\overline{\Gamma}_{\text{dB}}(x), C_{\text{dB}}(x))$. $\sum_{i=1}^{N} \alpha(x_i)$ is then the sum of lognormal random variables. As established in the literature, the lognormal distribution is a good approximation for the distribution of the sum of lognormal random variables [22]. Let α_{sum} with distribution $20\log_{10}\alpha_{\text{sum}} \sim \mathcal{N}(\mu_{\text{sum}}, \sigma_{\text{sum}}^2)$ denote the lognormal random variable approximating $\sum_{i=1}^{N}\alpha(x_i)$. μ_{sum} and σ_{sum}^2 can be found, based on $\overline{\Gamma}_{\text{dB}}(x)$ and $C_{\text{dB}}(x)$, by using the extended Fenton-Wilkinson (F-W) method [22]. The details are given in Appendix A. The outage probability inequality in (5) can then be expressed as $\mu_{\text{sum}} + \sigma_{\text{sum}} Q^{-1}(1 - \Pr_{\text{out}}) \geq 20\log_{10}(\alpha_{R,\text{th}})$, where $Q(.)$ denotes the Q function. Equation (5) can then be posed as

$$\begin{aligned} \underset{x}{\text{minimize}} \quad & \kappa_M \sum_i d_i(x_i) \\ \text{subject to} \quad & \mu_{\text{sum}} + \sigma_{\text{sum}} Q^{-1}(1 - \Pr_{\text{out}}) \geq 20\log_{10}\alpha_{R,\text{th}} \\ & x_i \in \mathcal{N}(x_i^0),\ i = 1, \cdots, N. \end{aligned} \tag{6}$$

We refer to this as the Motion Energy Stochastic Setting (MESS) minimization problem. The optimization problem (6) can then be solved by using existing optimization toolboxes. We next propose an alternative approach for the case of stochastic channel knowledge, based on our proposed MEMP approach of (3) of Section III-A.

1) Approximation using analysis of MEMP of (3): In Section III-A, we showed how the motion energy-aware optimization problem can be solved for the case of perfect channel knowledge. That analysis and the corresponding solution can be used to find an approximate solution for the stochastic case, as we show next. As introduced earlier, the channel power

[2] To predict the channel in transmission from any unvisited location to the remote station, the robots only need a small number of a priori channel measurements, $\Gamma_{q,\text{dB}}$, from which they can estimate the channel parameters ($\hat{\vartheta}$, $\hat{\beta}_{\text{SH}}$, $\hat{\nu}_{\text{SH}}$, $\hat{\nu}_{\text{MP}}$) [20]. If time division duplexing (TDD) is not utilized, the remote station can broadcast $\Gamma_{q,\text{dB}}$ to the unmanned vehicles during the operation, using a feedback channel. Alternatively, if we have TDD, then the robots can directly utilize a few a priori downlink channel samples to obtain $\Gamma_{q,\text{dB}}$.

in dB, $20\log_{10}\alpha(r_j)$, has the distribution $20\log_{10}\alpha(r_j) \sim \mathcal{N}\left(\mu(r_j), \sigma^2(r_j)\right)$, where r_j is the j^{th} cell, as defined in Section III-A, and $\mu(r_j) = \overline{\Gamma}_{\text{dB}}(r_j)$ and $\sigma^2(r_j) = C_{\text{dB}}(r_j)$ are obtained by evaluating Lemma 1 at $p = r_j$ (scalar). Consider $\tilde{\alpha}(r_j)$ such that $20\log_{10}\tilde{\alpha}(r_j) = \mu(r_j) - \zeta\sigma(r_j)$ for some constant $\zeta \geq 0$. $\tilde{\alpha}(r_j)$ provides a conservative estimate of the channel amplitude. We then approximate $\alpha(r_j)$ by $\tilde{\alpha}(r_j)$ in (3), which results in the following optimization problem:

$$\begin{aligned} \underset{\{z_{ij}\}}{\text{minimize}} \quad & J_{\text{MEMP}}(\{z_{ij}\}) \\ \text{subject to} \quad & \sum_i \sum_{j\in\mathcal{N}_i} \tilde{\alpha}(r_j) z_{ij} \geq \alpha_{R,\text{th}} \\ & \sum_{j\in\mathcal{N}_i} z_{ij} = 1,\ z_{ij} \in \{0,1\},\ \forall\, j \in \mathcal{N}_i,\ \forall\, i. \end{aligned} \tag{7}$$

Equation (7) can then be efficiently solved using the proposed approach of Section III-A for MEMP of (3). We next relate the optimization problem of (7) to the original optimization problem of (5) by finding a bound on the probability that the obtained solution satisfies the inequality constraint of (3). We first need the following lemma.

Lemma 3: $20\log_{10}\alpha(r_{j_i})$s are positively correlated as a result of the exponential correlation, where j_i is the cell chosen by robot i. We then have $\Pr\left(20\log_{10}\alpha(r_{j_i}) \geq \xi_i,\ \forall i\right) \geq \prod_{i=1}^N \Pr\left(20\log_{10}\alpha(r_{j_i}) \geq \xi_i\right)$, for any $\xi_i \in \mathbb{R}$.

Proof: See [23]. ■

Lemma 4: Let $\{z_{ij}\}$ be the solution of (7), and let j_i be such that $z_{ij_i} = 1$. Then the probability that this solution results in an outage in (3) is bounded as follows: $\Pr\left(\sum_{i=1}^N \alpha(r_{j_i}) < \alpha_{R,\text{th}}\right) < 1 - \left[Q\left(-\zeta\right)\right]^N$.

Proof: The probability of successful transmission is $\Pr\left(\sum_{i=1}^N \alpha(r_{j_i}) \geq \alpha_{R,\text{th}}\right) \geq \Pr\left(\sum_{i=1}^N \alpha(r_{j_i}) \geq \sum_{i=1}^N \tilde{\alpha}(r_{j_i})\right)$ since $\sum_{i=1}^N \tilde{\alpha}(r_{j_i}) \geq \alpha_{R,\text{th}}$ for a feasible solution of (7). Further, $\Pr\left(\sum_{i=1}^N \alpha(r_{j_i}) \geq \sum_{i=1}^N \tilde{\alpha}(r_{j_i})\right) \geq \Pr\left(20\log_{10}\alpha(r_{j_i}) \geq 20\log_{10}\tilde{\alpha}(r_{j_i}),\ \forall i\right) \geq \prod_{i=1}^N \Pr\left(\frac{20\log_{10}\alpha(r_{j_i}) - \mu(r_{j_i})}{\sigma(r_{j_i})} \geq -\zeta\right) = \left[Q\left(-\zeta\right)\right]^N$ where the second inequality follows from Lemma 3. ■

IV. Energy-Aware Cooperative Robotic Beamforming

In this section, we extend our results of Section III to include the communication energy cost as well, i.e., we are interested in finding the most energy efficient way (considering both motion and communication) for the robots to cooperatively transmit the data to a remote station. The robots need to determine new locations for transmission as well as the transmission powers such that they minimize the total energy consumption while satisfying the cooperative connectivity requirement. As in Section III, we start with the scenario of perfect channel knowledge, for which we obtain an ϵ-suboptimal solution by showing that solving our problem is equivalent to solving a series of multiple-choice knapsack problems. We then extend our analysis to the stochastic setting with probabilistic channel prediction and incorporate channel uncertainty into our formulation.

A. Perfect Channel Knowledge

In this case, the robots perform distributed transmit beamforming with complex weights $w_i = \rho_i e^{-\theta(x_i)}$, if node i moves to x_i, where $0 \leq \rho_i \leq 1$ and $\theta(x_i)$ is as described in Section II-C. The received power is then given as $P_R = P_0\left(\sum_{i=1}^N \alpha(x_i)\rho_i\right)^2$. As can be seen from Section II-B, imposing a minimum transmission rate requirement results in a minimum required received power which we denote by $P_{R,\text{th}}$ for a given $\eta_1, \eta_2 \leq 1$. For instance, in the case of uncoded MQAM, a bit error rate requirement of BER_{th}, results in $\eta_1 = 1$ and $\eta_2 = 1.5/\ln(5\text{BER}_{\text{th}})$, and a minimum spectral efficiency requirement would translate to a minimum required received power $P_{R,\text{th}}$. Imposing this results in $P_R = P_0\left(\sum_{i=1}^N \alpha(x_i)\rho_i\right)^2 \geq P_{R,\text{th}}$ or equivalently $\sum_{i=1}^N \alpha(x_i)\rho_i \geq \sqrt{\frac{P_{R,\text{th}}}{P_0}} = \alpha_{R,\text{th}}$, with $\rho_i^2 P_0$ denoting the transmit power of robot i.

The total energy cost is then given as $J_{\text{TE}}(x) = \kappa_M \sum_{i=1}^N d_i(x_i) + \frac{l P_0 \sum_{i=1}^N \rho_i^2}{\eta_1 B \log_2\left(1 + \eta_2 P_0 \frac{\left(\sum_{i=1}^N \alpha(x_i)\rho_i\right)^2}{N_0}\right)}$ and the resulting optimization problem can be expressed as

$$\begin{aligned} \underset{x,\rho}{\text{minimize}} \quad & J_{\text{TE}}(x) \\ \text{subject to} \quad & \sum_i \alpha(x_i)\rho_i \geq \alpha_{R,\text{th}} \\ & 0 \leq \rho_i \leq 1,\ x_i \in \mathcal{N}(x_i^0),\ i = 1, \cdots, N, \end{aligned} \tag{8}$$

where $\rho = \left[\rho_1 \cdots \rho_N\right]^{\text{T}}$, l is the number of bits to be transmitted to the remote station and $\mathcal{N}(x_i^0) \subseteq \mathcal{W}$ is the neighborhood around x_i^0 that robot i is constrained to be in.

As before, we first discretize the workspace $\mathcal{W}$ into M cells with centers $r_j \in \mathcal{W}$, for $j \in \{1, \cdots, M\}$. The optimization problem (8) can then be reformulated as

$$\begin{aligned} \underset{\{z_{ij}\},\rho}{\text{minimize}} \quad & J_{\text{TEMP}}(\{z_{ij}\}, \rho) \\ \text{subject to} \quad & \sum_i \sum_{j\in\mathcal{N}_i} \alpha(r_j)\rho_i z_{ij} \geq \alpha_{R,\text{th}} \\ & 0 \leq \rho_i \leq 1,\ i = 1, \cdots, N \\ & \sum_{j\in\mathcal{N}_i} z_{ij} = 1,\ z_{ij} \in \{0,1\},\ \forall\, j \in \mathcal{N}_i,\ \forall\, i, \end{aligned} \tag{9}$$

where $J_{\text{TEMP}}(\{z_{ij}\}, \rho) = \kappa_M \sum_{i=1}^N \sum_{j\in\mathcal{N}_i} d_i(r_j) z_{ij} + \frac{l P_0 \sum_{i=1}^N \rho_i^2}{\eta_1 B \log_2\left(1 + \eta_2 P_0 \frac{\left(\sum_i \sum_j \alpha(r_j)\rho_i z_{ij}\right)^2}{N_0}\right)}$, $d_i(r_j)$ is the distance to cell j for robot i, $\alpha(r_j)$ is the channel amplitude when transmitting from cell j to the remote station, and $\mathcal{N}_i \subseteq \{1, \cdots, M\}$ is the set of cells present in $\mathcal{N}(x_i^0)$. A value of $z_{ij} = 1$ implies that robot i moves to cell j. We refer to this problem as the Total Energy Minimization Problem (TEMP), with the optimal value of $J_{\text{TEMP}}^{\text{OPT}}$.

We begin by characterizing properties of the optimal communication strategy as well as of the optimal solution ($\{z_{ij}\}$,ρ) of TEMP of (9). This is one of the key intermediate steps that allows us to pose our problem as a series of multiple choice knapsack problems.

In the following lemma, we show that the inequality for the cooperative connectivity requirement in TEMP of (9) is satisfied with equality in the optimal solution.

Lemma 5: Let $(\{z_{ij}^{\text{OPT}}\}, \rho^{\text{OPT}})$ be an optimal solution of TEMP of (9). Let j_i^{OPT} be such that $z_{ij_i^{\text{OPT}}}^{\text{OPT}} = 1$. Then the solution satisfies $\sum_{i=1}^{N} \alpha(r_{j_i^{\text{OPT}}})\rho_i^{\text{OPT}} = \alpha_{R,\text{th}}$.

Proof: See Appendix B for the proof. ■

Next, consider the case where the positions of the robots are fixed and the only objective is to minimize the total transmit power (not energy) while satisfying the cooperative connectivity requirement. Lemma 6 characterizes the optimal solution of this case, as follows.

Lemma 6: Consider the following optimization problem:

$$\begin{aligned} \underset{\rho}{\text{minimize}} \quad & \sum_i \rho_i^2 \\ \text{subject to} \quad & \sum_i \alpha_i \rho_i \geq \alpha_{R,\text{th}} \\ & 0 \leq \rho_i \leq 1,\ i = 1, \cdots, N. \end{aligned} \tag{10}$$

The optimal solution for (10) is $\rho_i = \min\{\lambda\alpha_i, 1\}$ where $\lambda > 0$ is such that $\sum_i \min\{\lambda\alpha_i, 1\}\alpha_i = \alpha_{R,\text{th}}$.[3]

Proof: See Appendix C for the proof. ■

Using Lemma 5 and 6 as building blocks, we next characterize the optimal communication strategy of TEMP of (9) given the final optimal positions of the robots.

Lemma 7: Let $(\{z_{ij}^{\text{OPT}}\}, \rho^{\text{OPT}})$ be an optimal solution of TEMP of (9). Let j_i^{OPT} be such that $z_{ij_i^{\text{OPT}}}^{\text{OPT}} = 1$. Then $\rho_i^{\text{OPT}} = \min\{\lambda\alpha(r_{j_i^{\text{OPT}}}), 1\}$ where $\lambda > 0$ is such that $\sum_{i=1}^{N} \min\{\lambda\alpha(r_{j_i^{\text{OPT}}}), 1\}\alpha(r_{j_i^{\text{OPT}}}) = \alpha_{R,\text{th}}$.

Proof: We prove this by contradiction. Assume that $\rho_i^{\text{OPT}} \neq \rho_i^*$ where $\rho_i^* = \min\{\lambda\alpha(r_{j_i^{\text{OPT}}}), 1\}$, for $\lambda > 0$, such that $\sum_{i=1}^{N} \min\{\lambda\alpha(r_{j_i^{\text{OPT}}}), 1\}\alpha(r_{j_i^{\text{OPT}}}) = \alpha_{R,\text{th}}$. Then, $(\{z_{ij}^{\text{OPT}}\}, \rho^*)$ is a feasible solution of (9) since $\sum_{i=1}^{N} \alpha(r_{j_i^{\text{OPT}}})\rho_i^* = \alpha_{R,\text{th}}$. The cost of the optimal solution then becomes $J_{\text{TEMP}}(\{z_{ij}^{\text{OPT}}\}, \rho^{\text{OPT}}) = \kappa_M \sum_{i=1}^{N} d_i(r_{j_i^{\text{OPT}}}) + \kappa_C \sum_{i=1}^{N} (\rho_i^{\text{OPT}})^2 > \kappa_M \sum_{i=1}^{N} d_i(r_{j_i^{\text{OPT}}}) + \kappa_C \sum_{i=1}^{N} (\rho_i^*)^2 = J_{\text{TEMP}}(\{z_{ij}^{\text{OPT}}\}, \rho^*)$, following from Lemma 5 and Lemma 6, where $\kappa_C = \frac{lP_0}{\eta_1 B \log_2\left(1+\eta_2 \frac{P_{R,\text{th}}}{N_0}\right)}$. Thus, we have a contradiction, as we found a feasible solution with a lower cost. ■

We next pose an optimization problem motivated by Lemma 7, the solution to which will help us obtain the solution to TEMP of (9). Let $\kappa_C = \frac{lP_0}{\eta_1 B \log_2\left(1+\eta_2 \frac{P_{R,\text{th}}}{N_0}\right)}$, as was defined in Lemma 7. Consider the following optimization problem,

$$\begin{aligned} \underset{\{z_{ij}\},\lambda}{\text{minimize}} \quad & J_\lambda(\{z_{ij}\}, \lambda) \\ \text{subject to} \quad & \sum_i \sum_{j\in\mathcal{N}_i} \min\{\lambda\alpha(r_j), 1\}\,\alpha(r_j) z_{ij} \geq \alpha_{R,\text{th}} \\ & \sum_{j\in\mathcal{N}_i} z_{ij} = 1,\ z_{ij} \in \{0,1\},\ \forall\, j \in \mathcal{N}_i,\ \forall\, i, \end{aligned} \tag{11}$$

where $J_\lambda(\{z_{ij}\}, \lambda) = \kappa_M \sum_i \sum_{j\in\mathcal{N}_i} d_i(r_j) z_{ij} + \kappa_C \sum_i \sum_{j\in\mathcal{N}_i} \left[\min\{\lambda\alpha(r_j), 1\}\right]^2 z_{ij}$. We next show how to obtain an optimal solution for TEMP of (9) from an optimal solution for (11).

Lemma 8: Let $(\{z_{ij}^*\}, \lambda^*)$ be an optimal solution of (11). Let j_i^* be such that $z_{ij_i^*}^* = 1$ and let $\rho_i^* = \min\{\lambda^*\alpha(r_{j_i^*}), 1\}$. Then $(\{z_{ij}^*\}, \rho^*)$ is an optimal solution of TEMP of (9).

Proof: Without loss of generality, let λ^* be such that $\lambda^*\alpha(r_{j_i^*}) \leq 1$ for some i. We first show that the connectivity requirement inequality in (11) is satisfied with equality for the optimal solution, i.e., $\sum_{i=1}^{N} \min\{\lambda^*\alpha(r_{j_i^*}), 1\}\alpha(r_{j_i^*}) = \alpha_{R,\text{th}}$. We show this by contradiction. Assume otherwise, i.e., $\sum_{i=1}^{N} \min\{\lambda^*\alpha(r_{j_i^*}), 1\}\alpha(r_{j_i^*}) > \alpha_{R,\text{th}}$. Consider λ such that $\sum_{i=1}^{N} \min\{\lambda\alpha(r_{j_i^*}), 1\}\alpha(r_{j_i^*}) = \alpha_{R,\text{th}}$. Clearly we have $\lambda < \lambda^*$, which implies $\left[\min\{\lambda\alpha(r_{j_i^*}), 1\}\right]^2 < \left[\min\{\lambda^*\alpha(r_{j_i^*}), 1\}\right]^2$ for some i. Hence $J_\lambda(\{z_{ij}^*\}, \lambda) < J_\lambda(\{z_{ij}^*\}, \lambda^*)$, resulting in a contradiction. Thus $\sum_{i=1}^{N} \min\{\lambda^*\alpha(r_{j_i^*}), 1\}\alpha(r_{j_i^*}) = \alpha_{R,\text{th}}$.

Next, we show via contradiction that $(\{z_{ij}^*\}, \rho^*)$, obtained from an optimal solution of (11), is an optimal solution of TEMP of (9). Assume $(\{z_{ij}^*\}, \rho^*)$ is not an optimal solution of (9) and let $(z_{ij}^{\text{OPT}}, \rho^{\text{OPT}})$ be an optimal solution instead. From Lemma 7, we have that $\rho_i^{\text{OPT}} = \min\{\lambda^{\text{OPT}}\alpha(r_{j_i^{\text{OPT}}}), 1\}$, where $\lambda^{\text{OPT}} > 0$ is such that $\sum_{i=1}^{N} \min\{\lambda\alpha(r_{j_i^{\text{OPT}}}), 1\}\alpha(r_{j_i^{\text{OPT}}}) = \alpha_{R,\text{th}}$. Then, we have $J_{\text{TEMP}}(\{z_{ij}^{\text{OPT}}\}, \rho^{\text{OPT}}) = \kappa_M \sum_{i=1}^{N} d_i(r_{j_i^{\text{OPT}}}) + \kappa_C \sum_{i=1}^{N} \left[\min\{\lambda^{\text{OPT}}\alpha(r_{j_i^{\text{OPT}}}), 1\}\right]^2 = J_\lambda(\{z_{ij}^{\text{OPT}}\}, \lambda^{\text{OPT}})$, and similarly $J_{\text{TEMP}}(\{z_{ij}^*\}, \rho^*) = J_\lambda(\{z_{ij}^*\}, \lambda^*)$. As a result, $J_{\text{TEMP}}(\{z_{ij}^*\}, \rho^*) > J_{\text{TEMP}}(\{z_{ij}^{\text{OPT}}\}, \rho^{\text{OPT}})$ implies that $J_\lambda(\{z_{ij}^*\}, \lambda^*) > J_\lambda(\{z_{ij}^{\text{OPT}}\}, \lambda^{\text{OPT}})$. Thus, $(\{z_{ij}^{\text{OPT}}\}, \lambda^{\text{OPT}})$ is a feasible solution for (11) with a lower cost than $(\{z_{ij}^*\}, \lambda^*)$, resulting in a contradiction. ■

ϵ-Suboptimal Solution: In this subsection we pose a series of multiple-choice knapsack problems and relate their solution to TEMP of (9) to obtain an ϵ-suboptimal solution. In this context, ϵ is a positive variable that determines how close to the optimal solution we can get. Basically, for each fixed value of λ, we have a multiple-choice knapsack problem, as can be seen from (11), which we can solve optimally. We then discretize λ uniformly with ϵ determining the corresponding resolution. Let $\lambda_k = k\epsilon_1/\alpha_{\max}$ for $k \in \{T_1 - 1, \cdots, T_2 - 1\}$ and $\lambda_{T_2} = 1/\alpha_{\min}^0$, where $\epsilon_1 = \frac{\epsilon}{2N\left(\alpha_{\max}/\alpha_{\min}^0\right)}$, $\alpha_{\max} = \max_{j\in\{1,\cdots,M\}} \alpha(r_j)$ and $\alpha_{\min}^0 = \min\{\alpha(x_i^0) : i = 1, \cdots, N\}$ denotes the minimum channel amplitude among the initial positions of the robots. Furthermore, $T_1 = \left\lceil \frac{1}{\epsilon_1} \frac{\alpha_{R,\text{th}}}{N\alpha_{\max}} \right\rceil = \left\lceil \frac{2}{\epsilon} \frac{\alpha_{R,\text{th}}}{\alpha_{\min}^0} \right\rceil$ and $T_2 = \left\lceil \frac{1}{\epsilon_1} \frac{\alpha_{\max}}{\alpha_{\min}^0} \right\rceil = \left\lceil \frac{2N}{\epsilon} \left(\frac{\alpha_{\max}}{\alpha_{\min}^0}\right)^2 \right\rceil$ determine the range of λ, as explained next. Since $\sum_{i=1}^{N} \min\{\lambda\alpha(r_{j_i}), 1\}\alpha(r_{j_i}) \leq \sum_{i=1}^{N} (\lambda_{T_1-1}\alpha_{\max})\alpha_{\max} = \left(\left\lceil \frac{1}{\epsilon_1} \frac{\alpha_{R,\text{th}}}{N\alpha_{\max}} \right\rceil - 1\right)\epsilon_1 N\alpha_{\max} < \alpha_{R,\text{th}}$, $\lambda \leq \lambda_{T_1-1}$ could not be a feasible solution of (11). Moreover, an optimal solution $(\{z_{ij}^*\}, \lambda^*)$ would not involve a robot incurring motion energy to get to a location with a worse channel amplitude, resulting in $\alpha(r_{j_i^*}) \geq \alpha_{\min}^0\ \forall i$. Since $\lambda_{T_2}\alpha_{\min}^0 = 1$, we have that if $\lambda^* > \lambda_{T_2}$ is an optimal solution, then λ_{T_2} is also an optimal solution. Thus, we need to only consider $\lambda \in (\lambda_{T_1-1}, \lambda_{T_2}]$ in (11), which results in the

[3] In this case, α_i can be interpreted as the fixed channel amplitude from robot i to the remote station.

following optimization problem for each $k \in \{T_1, \cdots, T_2\}$:

$$\begin{aligned} &\underset{\{z_{ij}\}}{\text{minimize}} && J_{\lambda,k}(\{z_{ij}\}) \\ &\text{subject to} && \sum_i \sum_{j \in \mathcal{N}_i} \left[\min\{\lambda_k \alpha(r_j), 1\}\right] \alpha(r_j) z_{ij} \geq \alpha_{R,\text{th}} \\ &&& \sum_{j \in \mathcal{N}_i} z_{ij} = 1,\ z_{ij} \in \{0,1\},\ \forall\, j \in \mathcal{N}_i,\ \forall\, i, \end{aligned} \tag{12}$$

where $J_{\lambda,k}(\{z_{ij}\}) = \sum_i \sum_{j \in \mathcal{N}_i} (\kappa_M d_i(r_j) + \kappa_C \left[\min\{\lambda_k \alpha(r_j), 1\}\right]^2) z_{ij}$, with the optimum value of $J^{\text{OPT}}_{\lambda,k}$. This optimization problem can be solved similar to (3) by posing it as a knapsack problem through a change of variable as shown in Section III.

Let $J_{\lambda,\min} = \min_{k \in \{T_1, \cdots, T_2\}} \{J^{\text{OPT}}_{\lambda,k}\}$. In order to find $J_{\lambda,\min}$, we need to solve $T_2 - T_1 + 1 \leq \left\lceil \frac{2N}{\epsilon} \frac{\alpha_{\max}}{\alpha^0_{\min}} \left(\frac{\alpha_{\max}}{\alpha^0_{\min}} - \frac{\alpha_{R,\text{th}}}{N \alpha_{\max}} \right) \right\rceil + 1$ multiple choice knapsack problems. As can be seen, the number of knapsack problems to be solved grows linearly with N and $\frac{1}{\epsilon}$. In the following theorem, we show how we can get arbitrarily close to the optimal solution by solving this set of knapsack problems.

Theorem 1: Let $m = \arg\min_{k \in \{T_1, \cdots, T_2\}} \{J^{\text{OPT}}_{\lambda,k}\}$. Let $\{z^*_{ij}\}$ be a solution of (12) when $k = m$, and j^*_i be such that $z^*_{ij^*_i} = 1$. Consider a λ^* such that $\lambda^* \leq \lambda_m$ and $\sum_{i=1}^N \left[\min\{\lambda^* \alpha(r_{j^*_i}), 1\}\right] \alpha(r_{j^*_i}) = \alpha_{R,\text{th}}$. Further, set $\rho^*_i = \min\{\lambda^* \alpha(r_{j^*_i}), 1\}$. Then, $(\{z^*_{ij}\}, \rho^*)$ is a feasible solution of TEMP of (9) and

$$J_{\text{TEMP}}(\{z^*_{ij}\}, \rho^*) \leq J^{\text{OPT}}_{\text{TEMP}} + \epsilon \kappa_C. \tag{13}$$

Proof: It is straightforward to see that $(\{z^*_{ij}\}, \rho^*)$ is a feasible solution of TEMP of (9). Moreover, $J_{\text{TEMP}}(\{z^*_{ij}\}, \rho^*) = J_\lambda(\{z^*_{ij}\}, \lambda^*) \leq J_\lambda(\{z^*_{ij}\}, \lambda_m) = J^{\text{OPT}}_{\lambda,m} = J_{\lambda,\min}$ since $J_\lambda(.)$ is a non-decreasing function of λ.

Let $(\{z^{\text{OPT}}_{ij}\}, \lambda^{\text{OPT}})$ be an optimal solution of (11). From Lemma 8 we have that $J^{\text{OPT}}_{\text{TEMP}} = J_\lambda(\{z^{\text{OPT}}_{ij}\}, \lambda^{\text{OPT}})$. Let $\lambda^{\text{OPT}} \in (\lambda_{T_1-1}, \lambda_{T_2}]$, as we established earlier. Thus, there exists a $k \in \{T_1, \cdots, T_2\}$ such that $\lambda^{\text{OPT}} \in (\lambda_{k-1}, \lambda_k]$. We then have $J_{\text{TEMP}}(\{z^*_{ij}\}, \rho^*) \leq J_{\lambda,\min} \leq J^{\text{OPT}}_{\lambda,k} \leq J_\lambda(\{z^{\text{OPT}}_{ij}\}, \lambda_k) = J_\lambda(\{z^{\text{OPT}}_{ij}\}, \lambda^{\text{OPT}}) + \left(J_\lambda(\{z^{\text{OPT}}_{ij}\}, \lambda_k) - J_\lambda(\{z^{\text{OPT}}_{ij}\}, \lambda^{\text{OPT}})\right) \leq J^{\text{OPT}}_{\text{TEMP}} + \kappa_C \sum_{i=1}^N \left(\lambda_k^2 - (\lambda^{\text{OPT}})^2\right) \left(\alpha(r_{j^{\text{OPT}}_i})\right)^2 \leq J^{\text{OPT}}_{\text{TEMP}} + \kappa_C \sum_{i=1}^N (\lambda_k - \lambda_{k-1})(\lambda_k + \lambda_k) \left(\alpha(r_{j^{\text{OPT}}_i})\right)^2 \leq J^{\text{OPT}}_{\text{TEMP}} + 2\frac{\epsilon_1}{\alpha_{\max}} \lambda_{T_2} \kappa_C \sum_{i=1}^N \left(\alpha(r_{j^{\text{OPT}}_i})\right)^2 \leq J^{\text{OPT}}_{\text{TEMP}} + 2N\epsilon_1 \frac{\alpha_{\max}}{\alpha^0_{\min}} \kappa_C = J^{\text{OPT}}_{\text{TEMP}} + \epsilon \kappa_C$. ■

Remark 2: κ_C is the communication energy cost of a single robot when it transmits at maximum power and the robots satisfy the cooperative connectivity requirement with equality.

Remark 3: Solving TEMP of (9) through a brute-force search of space is infeasible even for moderately small values of the number of robots (N). For instance, if M is the number of points in the discretized workspace and if we represent each ρ_i by k bits, then the computational complexity of an exhaustive search is $M^N 2^{kN}$. On the other hand, with our proposed ϵ-suboptimal solution, the number of multiple-choice knapsack problems to solve grows linearly with N and $\frac{1}{\epsilon}$. We note that while we can solve (8) with an existing solver, there is no guarantee that the solver will find the global optimum since the objective function is non-convex. Theorem 1 then allows us to get arbitrarily close to the optimal solution with a low computational complexity.

B. Probabilistic Channel Prediction

As discussed earlier, in realistic scenarios, the unmanned vehicles do not know the uplink channel when transmitting from unvisited locations. As such, they will probabilistically predict the channel based on a small number of a priori measurements in the same environment, as summarized in Section II-D2. The energy-aware (both motion and communication) cooperative beamforming problem (8), can then be extended to the following in this stochastic setting:

$$\begin{aligned} &\underset{x,\rho}{\text{minimize}} && J_{\text{TE,ST}}(x, \rho) \\ &\text{subject to} && \Pr\Big(\sum_i \alpha(x_i)\rho_i < \alpha_{R,\text{th}}\Big) < \Pr_{\text{out}} \\ &&& 0 \leq \rho_i \leq 1,\ x_i \in \mathcal{N}(x^0_i),\ i = 1, \cdots, N, \end{aligned} \tag{14}$$

where $J_{\text{TE,ST}}(x, \rho) = \kappa_M \sum_{i=1}^N d_i(x_i) + \mathbb{E}\left[\frac{l P_0 \sum_i \rho_i^2}{\eta_1 B \log_2\left(1 + \eta_2 \frac{P_0 (\sum_i \alpha(x_i)\rho_i)^2}{N_0}\right)}\right]$, with $x = [x_1 \cdots x_N]^{\mathrm{T}}$ and $\rho = [\rho_1 \cdots \rho_N]^{\mathrm{T}}$ as optimization variables and $\mathbb{E}(.)$ representing the average of the argument. In this case, the average is taken over $\alpha(x_i)$, $\forall i$. The vector $[\alpha(x_1)\rho_1 \cdots \alpha(x_N)\rho_N]^{\mathrm{T}}$ is a lognormal random vector with distribution $[20\log_{10}(\alpha(x_1)\rho_1) \cdots 20\log_{10}(\alpha(x_N)\rho_N)]^{\mathrm{T}} \sim \mathcal{N}\left(\rho_{\text{dB}} + \overline{\Gamma}_{\text{dB}}(x), C_{\text{dB}}(x)\right)$ where $\overline{\Gamma}_{\text{dB}}(x)$ and $C_{\text{dB}}(x)$ are the estimated mean and covariance matrix of the predicted channel power respectively, and $[\rho_{\text{dB}}]_i = 20\log_{10}\rho_i$. Let $\alpha_{\text{sum},\rho}$ with distribution $20\log_{10}\alpha_{\text{sum},\rho} \sim \mathcal{N}(\mu_{\text{sum},\rho}, \sigma^2_{\text{sum},\rho})$ denote the lognormal random variable approximating $\sum_{i=1}^N \alpha(x_i)\rho_i$. $\mu_{\text{sum},\rho}$ and $\sigma^2_{\text{sum},\rho}$ can be found, based on ρ_{dB}, $\overline{\Gamma}_{\text{dB}}(x)$ and $C_{\text{dB}}(x)$, by using the extended Fenton-Wilkinson method [22]. Similar to Section III, the objective then becomes $J_{\text{TESS}}(x, \rho) = \kappa_M \sum_i d_i(x_i) + \mathbb{E}\left[\frac{l P_0}{\eta_1 B \log_2\left(1 + \eta_2 \frac{P_0 \alpha^2_{\text{sum},\rho}}{N_0}\right)} \sum_i \rho_i^2\right]$, and our optimization problem can be rewritten as

$$\begin{aligned} &\underset{x,\rho}{\text{minimize}} && J_{\text{TESS}}(x, \rho) \\ &\text{subject to} && \mu_{\text{sum},\rho} + \sigma_{\text{sum},\rho} Q^{-1}(1 - \Pr_{\text{out}}) \geq 20\log_{10}\alpha_{R,\text{th}} \\ &&& 0 \leq \rho_i \leq 1,\ i = 1, \cdots, N \\ &&& x_i \in \mathcal{N}(x^0_i),\ i = 1, \cdots, N, \end{aligned} \tag{15}$$

which can then be solved by using existing optimization toolboxes. We refer to this as the Total Energy Stochastic Setting (TESS) minimization problem.

1) Approximation using analysis of TEMP of (9): Similar to Lemma 4, the stochastic optimization problem of (14) can be approximately but efficiently solved using the solution to TEMP of (9), which is for the perfect channel knowledge case. As introduced earlier, the channel power in dB, $20\log_{10}\alpha(r_j)$, has the distribution $20\log_{10}\alpha(r_j) \sim \mathcal{N}\left(\mu(r_j), \sigma^2(r_j)\right)$, where r_j is the j^{th} cell, as defined in Section III-A, and $\mu(r_j) = \overline{\Gamma}_{\text{dB}}(r_j)$ and $\sigma^2(r_j) = C_{\text{dB}}(r_j)$ are obtained by evaluating Lemma 1 at $p = r_j$ (scalar). Consider $\tilde{\alpha}(r_j)$ such that $20\log_{10}\tilde{\alpha}(r_j) = \mu(r_j) - \zeta\sigma(r_j)$ for some constant $\zeta \geq 0$. $\tilde{\alpha}(r_j)$ provides a conservative estimate of the channel amplitude with a high probability. We then approximate $\alpha(r_j)$ by $\tilde{\alpha}(r_j)$ in (9), which results in the following optimization:

$$\begin{aligned} \underset{\{z_{ij}\},\rho}{\text{minimize}} \quad & \tilde{J}_{\text{TESS}}(\{z_{ij}\},\rho) \\ \text{subject to} \quad & \sum_i \sum_{j\in\mathcal{N}_i} \tilde{\alpha}(r_j)\rho_i z_{ij} \geq \alpha_{R,\text{th}} \\ & 0 \leq \rho_i \leq 1,\ i = 1,\cdots,N \\ & \sum_{j\in\mathcal{N}_i} z_{ij} = 1,\ z_{ij} \in \{0,1\},\ \forall\, j \in \mathcal{N}_i,\ \forall\, i. \end{aligned} \tag{16}$$

where $\tilde{J}_{\text{TESS}}(\{z_{ij}\},\rho) = \kappa_M \sum_i \sum_{j\in\mathcal{N}_i} d_i(r_j) z_{ij} + \frac{lP_0 \sum_i \rho_i^2}{\eta_1 B \log_2\left(1+\eta_2 P_0 \frac{\left(\sum_i \sum_{j\in\mathcal{N}_i} \tilde{\alpha}(r_j)\rho_i z_{ij}\right)^2}{N_0}\right)}$. Equation (16) can then be efficiently solved using the proposed approach of Section IV-A for TEMP. We next relate the optimization problem of (16) to the original optimization problem of (14) by finding a bound on the probability that the obtained solution satisfies the inequality constraint of (9).

Lemma 9: Let $(\{z_{ij}\},\rho)$ be the solution obtained when solving (16) using the proposed approach of Section IV-A, and let j_i be such that $z_{ij_i} = 1$. The probability that this solution results in an outage in (9) is bounded as follows: $\Pr\left(\sum_i \alpha(r_{j_i})\rho_i < \alpha_{R,\text{th}}\right) < 1 - \left[Q\left(-\zeta\right)\right]^N$.
The proof is similar to the proof of Lemma 4.

V. Simulation Results

Consider a scenario where 6 robots are located in a 50 m $\times$ 50 m workspace with the remote station at the origin and initial positions as shown in Fig. 5. The channel is generated using the probabilistic channel model described in Section II-D1, with the following parameters that were obtained from real channel measurements in downtown San Francisco [15] : $n_{\text{PL}} = 4.4$, $\nu_{\text{SH}} = 6.76$ and $\beta_{\text{SH}} = 22.6$ m. Moreover, the multipath fading is taken to be uncorrelated Rician fading with the parameter $K_{\text{ric}} = 3.9$. We consider a bandwidth of $B = 10$ MHz and the received noise power is taken to be a realistic value of -100 dBmW [24]. We consider uncoded MQAM modulation with a BER tolerance of 10^{-5} and a minimum spectral efficiency requirement (transmission rate divided by bandwidth) of[4] 4. This corresponds to $\eta_2 = 0.1515$ and a minimum received SNR requirement of 20 dB which, for the given noise power, corresponds to a received power requirement of $P_{R,\text{th,dBm}} = -80$ dBmW. We take the maximum transmission power of a node to be $P_{0,\text{dBm}} = 27$ dBmW [25], which results in $\alpha_{R,\text{th},dB} = -53.5$ dB. The amount of data to be transferred is 800 bits/Hz. The robots are situated far enough from the remote station that they do not satisfy the received power requirement at their initial positions (see Fig. 5). The neighborhood $\mathcal{N}_i$, within which the final position of robot i is constrained to lie in, is taken to be the entire workspace. The optimization problems of MEMP, MESS, TEMP and TESS, can be solved centrally by either one of the robots or by the remote station.

A. Perfect Channel Knowledge

We first analyze the trends of the motion energy-aware (MEMP) and the total energy-aware (TEMP) approaches as the communication load (l/B) varies in Figures 3, 4 and 5. TEMP of (9) is solved via the set of multiple-choice knapsack problems of Theorem 1 with $\epsilon = 0.05$. As shown in Theorem 1, the optimal value lies at most $0.05\kappa_C$ below the value obtained by solving the family of knapsack problems. This confidence bound is also shown in Fig. 3. It can be seen that the confidence bound is very close to the solution obtained by using Theorem 1 for solving TEMP, which confirms that Theorem 1 can get arbitrarily close to the optimal solution with a considerably low computational complexity. Each data point on the plots is obtained by averaging over 100 channels generated for the given set of channel parameters.

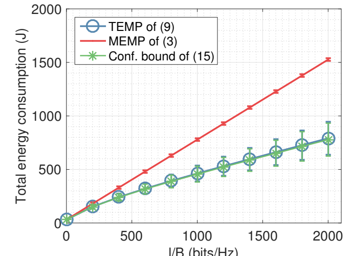

Fig. 3: Total energy (sum of motion and communication) consumption of MEMP and TEMP for different communication loads for the case of perfect channel knowledge. TEMP provides a considerable energy saving, as expected. MEMP refers to the case where only motion energy is minimized while communication energy is also adapted and co-optimized in TEMP.

Fig. 3 shows the average total energy consumption of MEMP and TEMP. The figure also shows the corresponding error bars, representing the standard deviation of the total energy consumption for each data point. As can be seen, TEMP provides a significant energy saving as the communication load l/B increases. In TEMP, with increasing l/B, the time for transmission increases as well, as a direct consequence of Lemma 5. Transmission power is thus penalized more and the robots travel larger distances to get to the locations with a better channel quality, allowing them to utilize a lower transmit power for communication. More specifically, Fig. 4 shows the total distance traveled as l/B varies. We can see that TEMP travels larger distances as l/B increases. Fig. 4 also shows how the total communication transmission power of TEMP decreases with increasing l/B. This is due to the fact that in TEMP, by incurring more motion energy, the nodes can find spots with a better channel quality, resulting in a lower communication energy and a lower total energy consumption. Fig. 5 shows the behavior of the solution of MEMP and TEMP for communication loads of $l/B = 100$ bits/Hz and $l/B = 1500$ bits/Hz. The background color encodes the channel power to the remote station. The lighter (darker) areas correspond to regions with better (worse) channel quality. As expected, the TEMP solution moves larger distances in the high communication load case to get to locations with a better channel quality.

B. Probabilistic Channel Prediction

We next consider the case where the channel is not known in the transmission from unvisited locations. We consider the workspace of Fig. 8. The robots are assumed to have 5% a priori channel measurements in this workspace. The robots then utilize the channel prediction framework of Section

[4]Note that the BER requirement is always satisfied, even if the minimum transmission rate requirement is not satisfied.

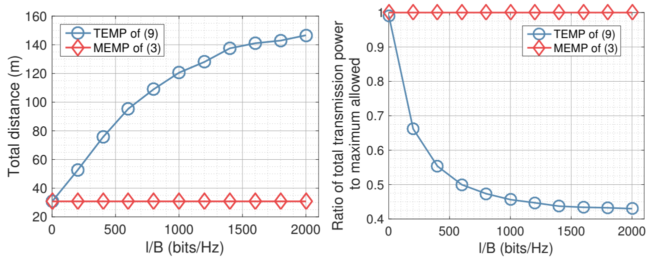

Fig. 4: Total (left) distance traveled and (right) transmission power utilized by MEMP and TEMP as a function of communication load and for the case of perfect channel knowledge.

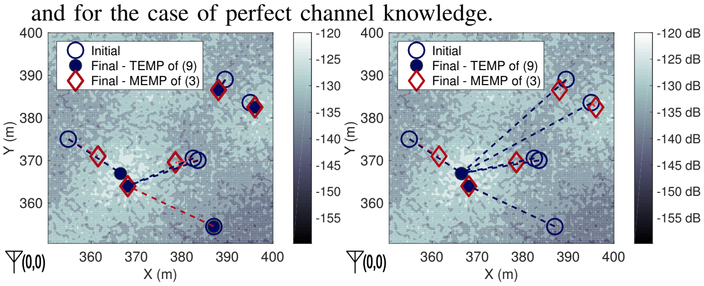

Fig. 5: Solution of MEMP and TEMP for (left) low ($l/B = 100$ bits/Hz) and (right) high ($l/B = 1500$ bits/Hz) communication loads for the case of perfect channel knowledge. The background represents the uplink channel power with lighter (darker) regions corresponding to a better (worse) channel quality. Readers are referred to the color pdf for a better viewing.

II-D2 for probabilistically predicting the channel at unvisited locations.[5] Channel and system parameters are as summarized earlier in this section, with $\text{Pr}_{\text{out}} = 0.2$. Fig. 6 shows the average total energy consumption as a function of l/B for both MESS and TESS. The figure also shows the corresponding error bars which represents the standard deviation of the total energy consumption for each data point. MESS refers to the case where only motion energy is minimized, for the case of probabilistic channel prediction, while communication energy is also adapted and co-optimized in TESS. Curves marked by TESS and MESS denote the total energy consumption when the nodes move to the final locations and experience the true channel values. The label 'TESS predicted' in Fig. 6, on the other hand, is obtained from (15) using predicted channel values and the lognormal approximation. In other words, the predicted curve is what the nodes predict to consume while the TESS curve is the true consumption. As expected, we see a significant performance improvement when using the total energy-aware approach (TESS), as compared to the motion energy-aware approach (MESS), especially as the communication load increases. Fig. 7 shows the total distance traveled by the robots for both MESS and TESS. Similar to the behavior of the perfect channel knowledge case, an increase in the communication load results in a larger penalization of the transmit power, and as a result TESS travels larger distances to get to locations with a better channel quality. Then TESS can use lower transmission powers, as can be seen in Fig. 7. Fig. 8 shows the behavior of MESS and TESS for communication loads of $l/B = 100$ bits/Hz and $l/B = 1500$ bits/Hz. The background color encodes the estimated channel power to the remote station. The lighter (darker) areas correspond to a better (worse) channel quality.

[5]MESS and TESS are solved using MATLAB's *fmincon* solver. *fmincon* requires the objective and the constraints to be twice differentiable and is thus unable to handle uncorrelated multipath. We then assume an exponentially correlated multipath in the channel predictor with a very small decorrelation distance of $\beta_{\text{MP}} = 0.033$ m, which has a negligible impact on the prediction performance. It should be noted that this is only for prediction purposes and that the real channel has an uncorrelated multipath.

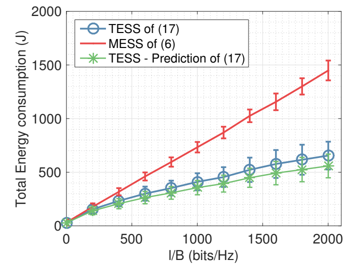

Fig. 6: Energy consumption of MESS and TESS for different communication loads for the case of probabilistic channel prediction. TESS provides a considerable energy saving, as expected. MESS refers to the case where only motion energy is minimized for the case of probabilistic channel prediction while communication energy is also adapted and co-optimized in TESS.

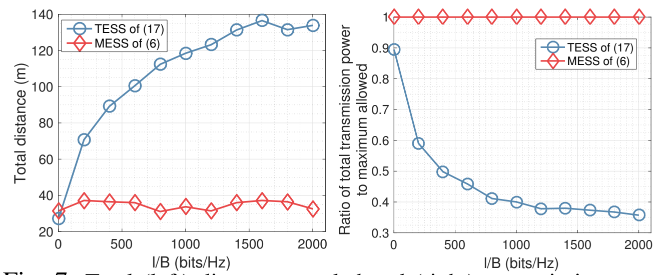

Fig. 7: Total (left) distance traveled and (right) transmission power utilized by MESS and TESS for different communication loads for the case of probabilistic channel prediction.

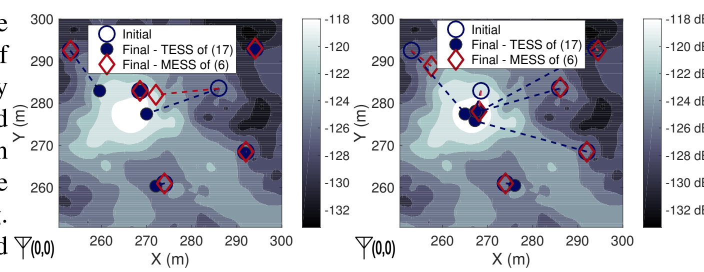

Fig. 8: Solution of MESS and TESS for (left) low ($l/B = 100$ bits/Hz) and (right) high ($l/B = 1500$ bits/Hz) communication loads for the case of probabilistic channel prediction. The background represents the estimated channel power with lighter (darker) regions corresponding to a better (worse) channel quality. Readers are referred to the color pdf for a better viewing.

Scenario	TESS of (15) with target $\text{Pr}_{\text{out}} = 0.2$	MESS of (6) with target $\text{Pr}_{\text{out}} = 0.2$	Approx. of (16) with $\zeta = 0.1$	Approx. of (7) with $\zeta = 0.1$
Prob. of outage	0.108	0.178	0.028	0.020

TABLE I: Probability of outage for TESS and MESS as well as for the approximations of (16) and (7) of Sections IV-B1 and III-B1. We can see that the target Pr_{out} is satisfied for TESS and MESS.

Remark 4 (Computational complexity): In our simulations, the implementation is done in MATLAB except for the MCKP solver, which is in C, and is adapted from David Pisinger's implementation [21]. The simulations were run on a 3.4 GHz i7-3770 CPU. For the case of Fig. 5, solving MEMP took 0.01 s, and solving TEMP took 25.2 s and 25.3 s for the case of low ($l/B = 100$ bits/Hz) and high ($l/B = 1500$ bits/Hz) communication loads respectively. For the case of Fig. 8 of probabilistic channel knowledge, solving MESS took 63.8 s and 53.2 s for the case of low ($l/B = 100$ bits/Hz) and high ($l/B = 1500$ bits/Hz) communication loads respectively. Furthermore, solving TESS took 122.7 s and 129.3 s for the case of low and high communication loads respectively.

Since the targeted outage probability was 0.2, some of the cases shown in Fig. 6 and 7 will result in outage, which means that the constraints of (9) and (3) will not be satisfied for TESS and MESS respectively. The first two columns of Table I show this outage probability, averaged over different communication loads, which is close to 0.2. In Sections III-B1 and IV-B1, we proposed an alternative way for solving the probabilistic cases by choosing $20\log_{10}\tilde{\alpha}(r_j) = \mu(r_j) - \zeta\sigma(r_j)$ in (7) and (16) with $\zeta \geq 0$, and utilizing the corresponding deterministic solutions. Table I also shows the probability of outage for such a case with $\zeta = 0.1$, for both the total energy-aware and motion energy-aware cases. We can see that this approach provides a good performance, with a low outage probability, in this case. The total energy consumption is also similar to TESS and MESS in these results. The computational complexity of this approach is also low, as it takes advantage of our proposed theories of Sections III-A and IV-A. Choosing ζ of $20\log_{10}\tilde{\alpha}(r_j) = \mu(r_j) - \zeta\sigma(r_j)$ in a methodical way, in order to satisfy a target probability of outage, is a subject of future work.

VI. Conclusions

In this paper, we considered a motion and communication co-optimization problem where a team of unmanned vehicles were tasked with cooperatively beamforming common information to a remote station in a realistic communication environment, while minimizing the total energy consumption (both motion and communication energy). For the case where the channel is known, we found an ϵ-suboptimal solution by proving that the original optimization problem can be posed as a series of multiple-choice knapsack problems. This solution provided the robots with the locations for distributed beamforming as well as the optimum transmission powers. We then extended our analysis and methodology to the case where the robots probabilistically predict the channel at unvisited locations. Finally, our simulation results showed the performance of the motion energy-aware and total energy-aware approaches for both perfect channel knowledge cases (MEMP and TEMP) as well as the stochastic cases (MESS and TESS). Overall, our results highlighted the underlying trends of the optimum strategy and indicated a considerable energy saving.

Appendix

A. Extended Fenton-Wilkinson Method

Consider a lognormal random vector $\alpha = [\alpha_1 \cdots \alpha_N]^{\mathrm{T}}$ with distribution $[20\log_{10}\alpha_1 \cdots 20\log_{10}\alpha_N]^{\mathrm{T}} \sim \mathcal{N}(\overline{\Gamma}_{\text{dB}}, C_{\text{dB}})$. The distribution can alternatively be expressed as $[\ln\alpha_1 \cdots \ln\alpha_N]^{\mathrm{T}} \sim \mathcal{N}(\mu, \Sigma)$, where $\mu = \xi\overline{\Gamma}_{\text{dB}}$, $\Sigma = \xi^2 C_{\text{dB}}$, and $\xi = 0.05\ln 10$. Let α_{sum} with distribution $20\log_{10}\alpha_{\text{sum}} \sim \mathcal{N}(\mu_{\text{sum}}, \sigma^2_{\text{sum}})$ denote the lognormal random variable approximating $\sum_i \alpha_i$. The first and second moments of $\sum_i \alpha_i$ are given by $u_1 = \mathbb{E}\left[\sum_i \alpha_i\right] = \sum_i e^{\mu_i + \Sigma_{ii}/2}$ and $u_2 = \mathbb{E}\left[\left(\sum_i \alpha_i\right)^2\right] = \sum_i e^{2\mu_i + 2\Sigma_{ii}} + 2\sum_{i=1}^{N-1}\sum_{j=i+1}^{N} e^{\mu_i+\mu_j} e^{\frac{1}{2}\left(\Sigma_{ii}+\Sigma_{jj}+2\Sigma_{ij}\right)}$), where μ_i is the i^{th} entry of μ and Σ_{ij} is the ij^{th} entry of Σ. In the extended Fenton-Wilkinson method [22], the first and second moments of α_{sum} and $\sum_i \alpha_i$ are equated to obtain $\mu_{\text{sum}} = \frac{1}{\xi}(2\ln(u_1) - \frac{1}{2}\ln(u_2))$ and $\sigma^2_{\text{sum}} = \frac{1}{\xi^2}\left(\ln(u_2) - 2\ln(u_1)\right)$.

B. Proof of Lemma 5

We first prove the following lemma, which we shall use in proving Lemma 5.

Lemma 10: Let $f : \mathbb{R}^n_+ \to \mathbb{R}_+$ with $f(\rho) = \frac{\sum_{i=1}^n \rho_i^2}{\ln\left(1+\xi\left(\sum_{i=1}^n \alpha_i\rho_i\right)^2\right)}$ where $\xi, \alpha_i > 0$. Given ρ, let $\mathcal{I} = \{i : \frac{\rho_i}{\alpha_i} \geq \frac{\rho_j}{\alpha_j} \forall j\}$ and let $v \in \mathbb{R}^n$ be such that its i^{th} element is $v(i) = \begin{cases} -\alpha_i, & \forall i \in \mathcal{I} \\ 0, & \text{else} \end{cases}$. Then $f(\rho)$ is strictly decreasing in direction v, i.e. $(\nabla f)^T v < 0$.

Proof:

$$\frac{\partial}{\partial\rho_k} f(\rho) = \frac{2\rho_k}{\ln\left(1+\xi\left(\sum_{i=1}^n \alpha_i\rho_i\right)^2\right)} - \frac{\left(\sum_{i=1}^n \rho_i^2\right) 2\xi\left(\sum_{i=1}^n \alpha_i\rho_i\right)\alpha_k}{\left(1+\xi\left(\sum_{i=1}^n \alpha_i\rho_i\right)^2\right)\left[\ln\left(1+\xi\left(\sum_{i=1}^n \alpha_i\rho_i\right)^2\right)\right]^2}. \tag{17}$$

Let $y = \xi\left(\sum_{i=1}^n \alpha_i\rho_i\right)^2$. Also, $\alpha_k\left(\sum_{i=1}^n \rho_i^2\right) = \rho_k\left(\sum_{i=1}^n \alpha_i\rho_i\right) + \sum_{i=1}^n \left(\alpha_k\rho_i - \alpha_i\rho_k\right)\rho_i$. Inserting this in (17) and rearranging result in $(\nabla f(\rho))^T v = \frac{2}{\ln(1+y)}\left\{\left(\sum_{k\in\mathcal{I}} -\alpha_k\rho_k\right)\left[1 - \frac{y}{(1+y)\ln(1+y)}\right] + \frac{\xi\left(\sum_{i=1}^n \alpha_i\rho_i\right)\left(\sum_{i=1}^n\left[\left(\sum_{k\in\mathcal{I}}\alpha_k^2\right)\rho_i - \alpha_i\left(\sum_{k\in\mathcal{I}}\alpha_k\rho_k\right)\right]\rho_i\right)}{(1+y)\ln(1+y)}\right\}$. We have $\frac{d}{dy}\left((1+y)\ln(1+y) - y\right) = \ln(1+y) > 0$ for $y > 0$. Also, $(1+y)\ln(1+y) - y|_{y=0} = 0$. Thus $(1+y)\ln(1+y) - y > 0$, which results in $\frac{y}{(1+y)\ln(1+y)} < 1$ for $y > 0$. Since $\frac{\rho_k}{\alpha_k} = \frac{\rho_j}{\alpha_j}, \forall j, k \in \mathcal{I}$, we have $\frac{\sum_{k\in\mathcal{I}}\alpha_k\rho_k}{\sum_{k\in\mathcal{I}}\alpha_k^2} = \frac{\alpha_j\rho_j + \sum_{k\in\mathcal{I},k\neq j}\alpha_k^2\frac{\rho_k}{\alpha_k}}{\sum_{k\in\mathcal{I}}\alpha_k^2} = \frac{\rho_j}{\alpha_j} \geq \frac{\rho_i}{\alpha_i}$, $\forall i$ for $j \in \mathcal{I}$. Thus, we have $\left(\sum_{k\in\mathcal{I}}\alpha_k^2\right)\rho_i - \alpha_i\left(\sum_{k\in\mathcal{I}}\alpha_k\rho_k\right) \leq 0$, $\forall i$, resulting in $(\nabla f(\rho))^T v < 0$. ■

Proof of Lemma 5: We prove this by contradiction. Assume that $\sum_{i=1}^N \alpha(r_{j_i^{\text{OPT}}})\rho_i^{\text{OPT}} > \alpha_{R,\text{th}}$. Let $\mathcal{I} = \{i : \frac{\rho_i}{\alpha(r_{j_i^{\text{OPT}}})} \geq \frac{\rho_k}{\alpha(r_{j_k^{\text{OPT}}})} \forall k\}$ and let $v \in \mathbb{R}^N$ be such that $v(i) = \begin{cases} -\alpha(r_{j_i^{\text{OPT}}}), & \forall i \in \mathcal{I} \\ 0, & \text{else} \end{cases}$. We decrease ρ in the direction of v until either $\frac{\rho_i}{\alpha(r_{j_i^{\text{OPT}}})} = \frac{\rho_k}{\alpha(r_{j_k^{\text{OPT}}})}$ for some $i \notin \mathcal{I}$ ($k \in \mathcal{I}$), or $\sum_i \alpha(r_{j_i^{\text{OPT}}})\rho_i = \alpha_{R,\text{th}}$. If $\frac{\rho_i}{\alpha(r_{j_i^{\text{OPT}}})} = \frac{\rho_k}{\alpha(r_{j_k^{\text{OPT}}})}$ for some $i \notin \mathcal{I}$ ($k \in \mathcal{I}$), we add i to $\mathcal{I}$, update our v, and continue decreasing ρ. If $\sum_i \alpha(r_{j_i^{\text{OPT}}})\rho_i = \alpha_{R,\text{th}}$, we terminate our update.

Let $\nabla_\rho J_{\text{TEMP}} = [\frac{\partial}{\partial\rho_1}J_{\text{TEMP}} \cdots \frac{\partial}{\partial\rho_N}J_{\text{TEMP}}]^{\mathrm{T}}$. From Lemma 10, we have $(\nabla_\rho J_{\text{TEMP}})^T v < 0$ and hence $J_{\text{TEMP}}(\{z_{ij}^{\text{OPT}}\}, \rho) < J_{\text{TEMP}}(\{z_{ij}^{\text{OPT}}\}, \rho^{\text{OPT}})$. Also, ρ is a feasible solution since $\sum_i \alpha(r_{j_i^{\text{OPT}}})\rho_i = \alpha_{R,\text{th}}$. We thus have a contradiction. ■

C. Proof of Lemma 6

Proof: We introduce Lagrange multipliers $\xi, \gamma \in \mathbb{R}^N$ for the inequality constraints $\rho_i \leq 1$ and $\rho_i \geq 0$ respectively, and $\lambda_0 \in \mathbb{R}$ for the constraint $\sum_i \alpha_i\rho_i \geq \alpha_{R,\text{th}}$. The Lagrangian is given as $L(\rho, \lambda_0, \xi, \gamma) = \sum_i \rho_i^2 + \sum_i \xi_i(\rho_i - 1) + \sum_i \gamma_i(-\rho_i) + \lambda_0 \left(\alpha_{R,\text{th}} - \sum_i \alpha_i \rho_i\right)$. We have the following KKT conditions:

$$2\rho_i^* - \lambda_0^* \alpha_i + \xi_i^* - \gamma_i^* = 0, \quad \xi_i^*(\rho_i^* - 1) = 0,$$
$$\gamma_i^* \rho_i^* = 0, \quad \lambda_0^*\big(\alpha_{R,\text{th}} - \sum_i \alpha_i \rho_i^*\big) = 0,$$
$$\xi^* \succeq 0, \quad \gamma^* \succeq 0, \quad \lambda_0^* > 0, \quad 0 \le \rho_i^* \le 1, \quad \sum_i \alpha_i \rho_i^* \ge \alpha_{R,\text{th}}.$$

Assume $\gamma_i^* > 0$ for some i. Then $\rho_i^* = 0$ and thus $\xi_i^* = 0$. But $\rho_i^* = \frac{\lambda_0^*}{2}\alpha_i - \frac{\xi_i^*}{2} + \frac{\gamma_i^*}{2} = \frac{\lambda_0^*}{2}\alpha_i + \frac{\gamma_i^*}{2} > 0$, resulting in a contradiction. Therefore, $\gamma_i^* = 0, \forall i$. Assume $\lambda_0^* = 0$. Then $\rho_i^* = -\frac{\xi_i^*}{2} = 0$, and hence $\sum_i \alpha_i \rho_i^* = 0 < \alpha_{R,\text{th}}$, resulting in a contradiction. Thus $\sum_i \alpha_i \rho_i^* = \alpha_{R,\text{th}}$. If $\frac{\lambda_0^*}{2}\alpha_i > 1$ then $\xi_i^* > 0$ which in turn implies that $\rho_i^* = 1$. If $\frac{\lambda_0^*}{2}\alpha_i < 1$, then $\xi_i^* = 0$ and hence $\rho_i^* = \frac{\lambda_0^*}{2}\alpha_i$. Thus, $\rho_i^* = \min\{\lambda\alpha_i, 1\}$, where $\lambda = \frac{\lambda_0^*}{2} > 0$ is such that $\sum_i \min\{\lambda\alpha_i, 1\}\alpha_i = \alpha_{R,\text{th}}$. ■

References

[1] A. Muralidharan and Y. Mostofi. Distributed beamforming using mobile robots. In *IEEE International Conference on Acoustics, Speech and Signal Processing (ICASSP)*, pages 6385–6389, 2016.

[2] Y. Yan and Y. Mostofi. Co-optimization of communication and motion planning of a robotic operation under resource constraints and in fading environments. *IEEE Transactions on Wireless Communications,*, 12(4):1562–1572, 2013.

[3] Y. Yan and Y. Mostofi. Robotic router formation in realistic communication environments. *IEEE Transactions on Robotics,*, 28(4):810–827, 2012.

[4] A. Ghaffarkhah and Y. Mostofi. Path planning for networked robotic surveillance. *IEEE Transactions on Signal Processing*, 60(7):3560–3575, July 2012.

[5] C. Dixon and E. Frew. Optimizing cascaded chains of unmanned aircraft acting as communication relays. *IEEE Journal on Selected Areas in Communications*, 30(5):883–898, 2012.

[6] N. Chatzipanagiotis, Y. Liu, A. Petropulu, and M. Zavlanos. Controlling groups of mobile beamformers. In *IEEE 51st Annual Conference on Decision and Control (CDC),*, pages 1984–1989, 2012.

[7] M. Stachura and E. Frew. Cooperative target localization with a communication-aware unmanned aircraft system. *Journal of Guidance, Control, and Dynamics*, 34(5):1352–1362, 2011.

[8] M. Lindhé and K. Johansson. Using robot mobility to exploit multipath fading. *IEEE Wireless Communications,*, 16(1):30–37, 2009.

[9] U. Ali, H. Cai, Y. Mostofi, and Y. Wardi. Motion and communication co-optimization with path planning and online channel prediction. In *American Control Conference (ACC)*, pages 7079–7084, 2016.

[10] A. Ghaffarkhah and Y. Mostofi. Channel learning and communication-aware motion planning in mobile networks. In *American Control Conference (ACC)*, pages 5413 –5420, 2010.

[11] Arjun Muralidharan and Yasamin Mostofi. First passage distance to connectivity for mobile robots. In *American Control Conference (ACC)*, pages 1517–1523, 2017.

[12] R. Mudumbai, D. Brown III, U. Madhow, and H. Poor. Distributed transmit beamforming: challenges and recent progress. *IEEE Communications Magazine,*, 47(2):102–110, 2009.

[13] P. Ochiai, H.and Mitran, H. Poor, and V. Tarokh. Collaborative beamforming for distributed wireless ad hoc sensor networks. *IEEE Transactions on Signal Processing,*, 53(11):4110–4124, 2005.

[14] J. Hou, Z. Lin, W. Xu, and G. Yan. Distributed transmit beamforming with autonomous and self-organizing mobile antennas. In *IEEE Global Telecommunications Conference*, pages 1–5, 2010.

[15] W. Smith and D. Cox. Urban propagation modeling for wireless systems. Technical report, DTIC Document, 2004.

[16] D. Goldenberg, J. Lin, A. Morse, B. Rosen, and Y. Yang. Towards mobility as a network control primitive. In *ACM international symposium on Mobile ad hoc networking and computing*, pages 163–174, 2004.

[17] C. Ooi and C. Schindelhauer. Minimal energy path planning for wireless robots. *Mobile Networks and Applications*, 14(3):309–321, 2009.

[18] C. Hsu. *Design and analysis of capacity-achieving codes and optimal receivers with low complexity*. PhD thesis, University of Michigan, 2006.

[19] A. Goldsmith. *Wireless communications*. Cambridge university press, 2005.

[20] M. Malmirchegini and Y. Mostofi. On the spatial predictability of communication channels. *IEEE Transactions on Wireless Communications,*, 11(3):964–978, 2012.

[21] D. Pisinger. A minimal algorithm for the multiple-choice knapsack problem. *European Journal of Operational Research*, 83(2):394–410, 1995.

[22] Adnan Abu-Dayya and Norman C Beaulieu. Outage probabilities in the presence of correlated lognormal interferers. *IEEE Transactions on Vehicular Technology,*, 43(1):164–173, 1994.

[23] J. Esary, F. Proschan, and D. Walkup. Association of random variables, with applications. *The Annals of Mathematical Statistics*, 38(5):1466–1474, 1967.

[24] K. Du and M. Swamy. *Wireless communication systems: from RF subsystems to 4G enabling technologies*. Cambridge University Press, 2010.

[25] S. Lönn, U. Forssen, P. Vecchia, Al Ahlbom, and M. Feychting. Output power levels from mobile phones in different geographical areas; implications for exposure assessment. *Occupational and Environmental Medicine*, 61(9):769–772, 2004.

Arjun Muralidharan received the Bachelors degree in Electronics and Communication Engineering from the Indian Institute of Technology, Guwahati, in 2012 and the MS degree in Electrical and Computer Engineering (ECE) from the University of California, Santa Barbara (UCSB) in 2014. He is currently working towards his PhD degree in the Department of Electrical and Computer Engineering at the University of California Santa Barbara. His research interests include cooperative robotic networks, game theory, wireless communications and information theory.

Yasamin Mostofi received the BS degree in electrical engineering from Sharif University of Technology, Tehran, Iran, in 1997, and the MS and PhD degrees from Stanford University, California, in 1999 and 2004, respectively. She is currently a professor in the Department of Electrical and Computer Engineering at the University of California Santa Barbara.

Dr. Mostofi is the recipient of 2016 Antonio Ruberti Prize from IEEE Control Systems Society, the Presidential Early Career Award for Scientists and Engineers (PECASE), the National Science Foundation (NSF) CAREER award, and the IEEE 2012 Outstanding Engineer Award of Region 6, among other awards. Her research is on mobile sensor networks. Current research thrusts include communication-aware robotics, human-robot networks, RF sensing, X-ray vision for robots, see-through imaging, and occupancy estimation. Her research has appeared in several reputable news outlets such as BBC, Huffington Post, Daily Mail, Engadget, and NSF Science360. She has served on the IEEE Control Systems Society conference editorial board 2008-2013. She is currently an associate editor for the IEEE TRANSACTIONS ON CONTROL OF NETWORK SYSTEMS. She is a senior member of the IEEE.